Hydrogen-Initiated Reactions of $(\mu\text{-H})_2Os_3(CO)_{10}$ with $[Mo(\eta^5\text{-}C_5H_5)(CO)_n]_2$ (n = 2, 3): Formation and Crystal Structures of Pentanuclear and Tetranuclear Clusters

Leh-Yeh Hsu, Wen-Liang Hsu, Deng-Yang Jan, and Sheldon G. Shore*

Department of Chemistry, The Ohio State University, Columbus, Ohio 43210

Received September 30, 1985

Molybdenum–osmium mixed-metal clusters $(\mu\text{-H})_2(\eta^5\text{-}C_5H_5)_2Mo_2Os_3(CO)_{12}$ (I), $(\mu\text{-H})_3(\eta^5\text{-}C_5H_5)MoOs_3(CO)_{11}$ (II), and $(\mu\text{-H})(\eta^5\text{-}C_5H_5)MoOs_3(CO)_{14}$ (III) were prepared through the hydrogen-initiated reaction between $(\mu\text{-H})_2Os_3(CO)_{10}$ and $[(\eta^5\text{-}C_5H_5)Mo(CO)_n]_2$ (n = 2, 3) at 90 °C. Relative yields of products appear to be a function of the effective hydrogen concentration. At 1 atm of H_2 in a static system the pentanuclear cluster I is the favored product while at 9 atm of H_2 the tetranuclear cluster II is favored. Yields of products appear to be independent of whether the starting material is the saturated or unsaturated molybdenum dimer. The crystal structures of $I\cdot C_6H_6$ and II have been determined. Compound $I\cdot C_6H_6$ (−15 °C): monoclinic, space group $P2_1/n$; a = 10.731 (2) Å, b = 19.583 (2) Å, c = 14.738 (2) Å, β = 93.65 (1)°, V = 3090.97 Å^3, Z = 4. Compound II (28 °C): monoclinic, space group $P2_1/c$; a = 16.545 (3) Å, b = 14.568 (5) Å, c = 18.288 (7) Å, β = 103.02 (3)°, V = 4294.66 Å^3, Z = 8. Structural analyses are based on 4315 independent reflections for compound I and 5580 independent reflections for compound II with $I > 3.0\sigma(I)$ collected on a diffractometer over the range $4° \le 2\theta \le 50°$. Final R_F and R_{wF} values are 2.4 and 3.5% for compound I and 3.6 and 4.8% for compound II. Compound I has C_s symmetry. The metals are in a trigonal-bipyramidal arrangement with a Mo_2Os triangle capped by Os atoms. Cluster II contains a tetrahedral arrangement of metal atoms. Carbon-13 NMR spectra of I and II are consistent with their solid-state structures.

Introduction

Reactions of the unsaturated cluster $(\mu\text{-H})_2Os_3(CO)_{10}$ with the metal carbonyls $Fe_2(CO)_9$, $Co_2(CO)_8$, $Co(\eta^5\text{-}C_5H_5)(CO)_2$, and $[Ni(\eta^5\text{-}C_5H_5)(CO)]_2$ have proved to be useful in the syntheses of tetranuclear mixed-metal clusters.[1-6] It has been suggested[1] that these metal carbonyls form unsaturated, active, metal carbonyl fragments under the thermal conditions employed in the syntheses and that these fragments add to the four-electron hydrogen-bridged system of $(\mu\text{-H})_2Os_3(CO)_{10}$ which is analogous to an olefinic bond. Owing to the relatively labile character of metal–metal bonds of first-row transition-metal carbonyl compounds compared to those in $(\mu\text{-H})_2Os_3(CO)_{10}$, these reactions lead to tetranuclear clusters containing an MOs_3 tetrahedron, where M is the first-row metal.

In the present study we have explored reactions of the second-row transition-metal dimers $[Mo(\eta^5\text{-}C_5H_5)(CO)_2]_2$ and $[Mo(\eta^5\text{-}C_5H_5)(CO)_3]_2$ with $(\mu\text{-H})_2Os_3(CO)_{10}$. In view of the greater strength of the metal–metal bond in these dimers compared to the examples cited above, it was of interest to determine if reactions could be induced and to determine if the metal–metal bond would be retained in any of the products. Although there is no apparent reaction in the absence of H_2,[7] we found that in the presence of H_2 a pentanuclear cluster, $(\mu\text{-H})_2(\eta^5\text{-}C_5H_5)_2Mo_2Os_3(CO)_{12}$ (I), and two tetranuclear clusters, $(\mu\text{-H})_3(\eta^5\text{-}C_5H_5)MoOs_3(CO)_{11}$ (II) and $(\mu\text{-H})(\eta^5\text{-}C_5H_5)MoOs_3(CO)_{14}$ (III), formed. These reactions give the first example of a pentanuclear cluster, I, obtained in this way. Reported here are the preparation of these clusters, the effect of H_2 concentration on the of distribution of products, and the crystal structures and NMR spectra of I and II.

Table I. Product Distributions from H_2-Initiated Reactions of $(\mu\text{-H})_2Os_3(CO)_{10}$ with $[Mo(\eta^5\text{-}C_5H_5)(CO)_2]_2$ and $[Mo(\eta^5\text{-}C_5H_5)(CO)_3]_2$

	conditions	% yield I	II	III
$[Mo(\eta^5HC_5H_5)(CO)_2]_2$	H_2 (1 atm) nonflow	23	trace	4
$[Mo(\eta^5\text{-}C_5H_5)(CO)_3]_2$	H_2 (1 atm) nonflow	21	9	2
$[Mo(\eta^5\text{-}C_5H_5)(CO)_2]_2$	H_2 (1 atm) flow through soln	14	15	trace
$[Mo(\eta^5\text{-}C_5H_5)(CO)_3]_2$	H_2 (1 atm) flow through soln	7	11	6
$[Mo(\eta^5\text{-}C_5H_5)(CO)_2]_2$	H_2 (9 atm) nonflow	trace	9	
$[Mo(\eta^5\text{-}C_5H_5)(CO)_3]_2$	H_2 (9 atm) nonflow	trace	11	trace

Experimental Section

Preparation of $(\mu\text{-H})_2(\eta^5\text{-}C_5H_5)_2Mo_2Os_3(CO)_{12}$, $(\mu\text{-H})_3(\eta^5\text{-}C_5H_5)MoOs_3(CO)_{11}$, and $(\mu\text{-H})(\eta^5\text{-}C_5H_5)MoOs_3(CO)_{14}$. The starting materials $(\mu\text{-H})_2Os_3(CO)_{10}$[8] and $[(\eta^5\text{-}C_5H_5)Mo(CO)_2]_2$[9] were prepared according to published methods while $[(\eta^5\text{-}C_5H_5)Mo(CO)_3]_2$ was purchased from Strem Chemicals and used without further purification. Toluene was dried over sodium and stored in a vessel in the presence of Na/benzophenone.

Both $(\mu\text{-H})_2Os_3(CO)_{10}$ (0.059 mmol) and $[(\eta^5\text{-}C_5H_5)Mo(CO)_2]_2$ (0.104 mmol) were weighed into a 50-mL three-necked round-bottom flask which was equipped with a condenser and a glass gas inlet tube. Freshly distilled toluene (10 mL) was then syringed into the vessel under a stream of hydrogen gas. Subsequently, the solution was kept at 90 °C with a small stream of H_2 bubbling through the reaction solution. The reaction was monitored by a TLC spot check from time to time and was stopped after 105

(1) Plotkin, J. S.; Alway, D. G.; Weisenberger, C. R.; Shore, S. G. *J. Am. Chem. Soc.* **1980**, *102*, 6157.
(2) Churchill, M. R.; Bueno, C.; Hsu, W.-L; Plotkin, J. S; Shore, S. G. *Inorg. Chem.* **1982**, *21*, 1958.
(3) Hsu, L.-Y.; Hsu, W.-L.; Jan, D.-Y.; Marshall, A. G.; Shore, S. G. *Organometallics* **1984**, *3*, 591.
(4) Shore, S. G.; Hsu, W.-L.; Weisenberger, C. R.; Caste, M. L.; Churchill, M. R.; Bueno, C. *Organometallics* **1982**, *1*, 1405.
(5) Shore, S. G.; Hsu, W.-L.; Churchill, M. R.; Bueno, C. *J. Am. Chem. Soc.* **1983**, *105*, 655.
(6) Churchill, M. R.; Bueno, C.; Kennedy, S.; Bricker, J. C.; Plotkin, J. S.; Shore, S. G. *Inorg. Chem.* **1982**, *21*, 627.
(7) Curtis, D.; Messerle, L.; Fotinos, N. A.; Gerlach, R. F. In *Reactivity of Metal-Metal Bonds*; Chisholm, M. H., Ed., ACS Symposium Series 155; American Chemical Society: Washington, DC, 1981.
(8) Knox, S. A. R.; Koepke, J. W.; Andrews, M. A.; Kaesz, H. D. *J. Am. Chem. Soc.* **1975**, *97*, 3942.
(9) Klingler, R. J.; Butler, W.; Curtis, M. D. *J. Am. Chem. Soc.* **1975**, *97*, 3535.

0276-7333/86/2305-1041$01.50/0

Table II. Crystallographic Data for $(\mu\text{-H})_2(\eta^5\text{-}C_5H_5)_2Mo_2Os_3(CO)_{12}\cdot C_6H_6$ (I) and $(\mu\text{-H})_3(\eta^5\text{-}C_5H_5)MoOs_3(CO)_{11}$ (II)

	I	II
chemical formula	$H_{13}Mo_2Os_3C_{23}O_{12}$	$H_3MoOs_3C_{16}O_{11}$
mol wt	1308.93	1042.8
color of cryst	black	orange
space group	$P2_1/n$	$P2_1/c$
molecules/unit cell	4	8
temp, °C	−15	28
a, Å	10.731 (2)	16.545 (3)
b, Å	19.583 (2)	14.568 (5)
c, Å	14.738 (2)	18.288 (7)
β, deg	93.65 (1)	103.02 (3)
vol, unit cell Å^3	3090.97	4294.66
cryst dimens, mm	0.175 × 0.275 × 0.275	0.15 × 0.25 × 0.50
D(calcd), g cm^{-3}	2.81	3.22
radiatn	Mo Kα (0.710 730 Å)	Mo Kα (0.710 730 Å)
absorptn coeff, cm^{-1}	131.39	183.07
max transmissn, %	99.98	99.99
min transmissn, %	50.45	38.75
scan mode	ω–2θ	ω–2θ
data collectn limits, deg	4–50	4–50
no. of unique reflctns	5425	8175
no. of reflctns used in structure refinement ($>3\sigma(I)$)	4315	5579
$R_F = \sum\|\|F_o\| - \|F_c\|\|/\|F_o\|$	0.024	0.036
$R_{wF} = \{\sum w(\|F_o\| - \|F_c\|)^2/w\|F_o\|^2\}^{1/2}$	0.035	0.048
$w = [\sigma(I)^2 + (kI)^2]^{-1/2}$	k = 0.03	k = 0.03

h. Toluene was removed under high vacuum to leave a dark brown residue. The residue was dissolved in a minimum amount of CH_2Cl_2 and chromatographed on a thin-layer plate (2-mm silica gel). Elution with 1/4 benzene–hexane gave four bands. In order of decreasing R_f values, these bands were yellow, pink, orange, and reddish brown.

The yellow band was identified as $(\mu\text{-H})(\eta^5\text{-}C_5H_5)MoOs_3(CO)_{14}$ (III) (2% yield based on $(\mu\text{-H})_2Os_3(CO)_{10}$) on the basis of its FT/ICR mass spectrum, obtained with a Nicolet FT/MS-1000 Fourier transform ion cyclotron resonance mass spectrometer equipped with a 3.0 T magnet and a 1-in. cubic cell (for parent ion peak $^1H_6{}^{12}C_{19}{}^{16}O_{14}{}^{98}Mo^{192}Os_3$ m/e(calcd) 1131.88, m/e(obsd) 1131.97), and its ^1H NMR spectrum. The infrared spectrum [ν(CO)] in cyclohexane is 2072 s, 2058 vs, 2048 s, 2028 m, 2018 s, 2008 m, and 1990 w (sh) cm^{-1}.

The pink band was identified as $[(\eta^5\text{-}C_5H_5)Mo(CO)_3]_2$ by its infrared spectrum.

The orange band was identified as $(\mu\text{-H})_3(\eta^5\text{-}C_5H_5)MoOs_3(CO)_{11}$ (II) (15% based on $(\mu\text{-H})_2Os_3(CO)_{10}$) from a single-crystal X-ray structure determination. Single crystals of $(\mu\text{-H})_3(\eta^5\text{-}C_5H_5)MoOs_3(CO)_{11}$ were obtained by crystallization from CH_2Cl_2/hexane at −15 °C. The infrared spectrum [ν(CO)] in cyclohexane is 2082 s, 2046 vs, 2008 m, 1999 m, 1962 w, and 1953 s cm^{-1}.

The reddish brown band (14% based on $(\mu\text{-H})_2Os_3(CO)_{10}$) was identified as $(\mu\text{-H})_2(\eta^5\text{-}C_5H_5)_2Mo_2Os_3(CO)_{12}$ (I) through an X-ray structural analysis at −15 °C. Crystals of $(\mu\text{-H})_2(\eta^5\text{-}C_5H_5)_2Mo_2Os_3(CO)_{12}\cdot C_6H_6$ were grown in a pentane/benzene mixed-solvent system at −15 °C. The infrared spectrum of $(\mu\text{-H})_2(\eta^5\text{-}C_5H_5)_2Mo_2Os_3(CO)_{12}$ [ν(CO)] in hexane is 2079 vw, 2068 w, 2042 vs, 2023 s, 1995 s, 1986 m, 1960 vw, 1945 vw, and 1842 w cm^{-1}.

When the preparative procedure was carried out with 1 atm of hydrogen over the reaction solution instead of bubbling hydrogen through the solution, a different product distribution was obtained: I (23%), II (2%), and III (4%).

The above syntheses were also started from $[(\eta^5\text{-}C_5H_5)Mo(CO)_3]_2$ by following the same procedures described above. Results are summarized in Table I.

Formation of $(\mu\text{-H})_3(\eta^5\text{-}C_5H_5)MoOs_3(CO)_{11}$ under Elevated H_2 Pressure. A toluene solution of $(\mu\text{-H})_2Os_3(CO)_{10}$ (0.176 mmol) and $[(\eta^5\text{-}C_5H_5)Mo(CO)_2]_2$ (0.245 mmol) was loaded to the 300-mL glass liner in a general purpose bomb (Parr Instrument Co.) in the nitrogen box. The system was then flushed with H_2 through several cycles of pressurizing the bomb with H_2 and then releasing the H_2. It was then pressurized to 9 atm, and the temperature was raised to 90 °C and maintained for 77 h with stirring. The pressure was then released, and the solvent was removed on a rotary evaporator leaving a reddish brown residue which was worked up according to the procedure described above. Cluster II was isolated in 9% yield while I was obtained in trace amount (Table I). Starting from $[(\eta^5\text{-}C_5H_5)Mo(CO)_3]_2$ gave an 11% yield of II and trace amounts of I and III (Table I).

Infrared and NMR Spectra. Infrared spectra of solutions in matched cells were recorded on a Perkin-Elmer 457 spectrometer and were calibrated by using polystyrene as a standard. Proton and carbon-13 NMR spectra were obtained on a Bruker WH-300 spectrometer at 300.13 and 75.4 mHz, respectively. Chemical shifts are referred to $Si(CH_3)_4$ (^1H, δ 0.00; ^{13}C, δ 0.00).

Carbon-13-enriched samples of I and II for ^{13}C NMR spectra were prepared from enriched $(\mu\text{-H})_2Os_3(CO)_{10}$ (ca. 25% ^{13}C) by using the preparative procedures described above. A known amount of $Os_3(CO)_{12}$ was enriched by stirring it in refluxing toluene under a known amount of CO (95%, ^{13}C, 1 atm of pressure) for 4 days at 110 °C. Extent of ^{13}CO enrichment of $Os_3(CO)_{12}$ was determined by mass spectral comparison of the ^{13}C content of the residual CO gas. The enriched $Os_3(CO)_{12}$ was then converted into $(\mu\text{-H})_2Os_3(CO)_{10}$.

Crystal Structure Determinations. For X-ray examination and data collection, each crystal was mounted at the tip of a thin glass fiber. All X-ray data were collected on a Enraf-Nonius CAD-4 diffractometer with graphite-monochromated Mo Kα radiation, and all the crystallographic computations were carried out on a PDP 11/44 computer using SDP (Structure Determination Package).[10] Table II gives crystallographic data for compounds I and II.

For each crystal, unit-cell parameters were obtained by least-squares refinement of the angular setting from 24 reflections, well distributed in reciprocal space and lying in a 2θ range of 15–30°. Intensity data were collected in the ω–2θ scan mode with a 2θ range of 4–50°. Six standard reflections were monitored and showed no significant decay. The data were corrected for Lorentz and polarization effects. The intensities were also corrected for absorption by using an empirical method based on the crystal orientation and measured ψ scans.

Both structures were solved by a combination of the direct method MULTAN 11/82 and the difference Fourier technique, and they were refined by full-matrix least squares. Analytical atomic scattering factors were used throughout the structure refinement with both the real and imaginary components of the anomalous dispersion included for all atoms. The heavy atoms first appeared on the E map. Then the positions of carbon and oxygen atoms were determined from a Fourier synthesis which

(10) SDP developed by B. A. Frenz and Associates, Inc., College Station, TX 77840, was used to process X-ray data, apply corrections, solve and refine and structure, produce drawings, and print tables.

(11) Churchill, M. R.; Hollander, F. J.; Shapley, J. R.; Foose, D. S. *J. Chem. Soc., Chem. Commun.* **1978**, 534.

Table III. Atomic Coordinates and Isotropic Thermal Parameters for $(\mu\text{-}H)_2(\eta^5\text{-}C_5H_5)_2Mo_2Os_3(CO)_{12}\cdot C_6H_6$[a] (Esd's in Parentheses)

atom	x	y	z	B, Å²
Os(1)	0.24934 (3)	0.18523 (1)	0.55645 (2)	1.754 (5)
Os(2)	0.44822 (3)	0.16891 (2)	0.43966 (2)	2.120 (6)
Os(3)	0.02211 (3)	0.22715 (2)	0.46465 (2)	2.043 (6)
Mo(4)	0.25740 (6)	0.27026 (3)	0.39552 (4)	1.85 (1)
Mo(5)	0.18836 (6)	0.12038 (3)	0.38786 (4)	1.86 (1)
O(11)	0.3183 (6)	0.3166 (3)	0.6567 (4)	3.6 (1)
O(12)	0.0672 (7)	0.1439 (4)	0.6964 (4)	5.3 (2)
O(13)	0.4294 (6)	0.1023 (4)	0.6811 (4)	4.9 (2)
O(21)	0.5903 (6)	0.0547 (4)	0.5406 (5)	6.0 (2)
O(22)	0.6137 (6)	0.2786 (3)	0.5321 (4)	4.6 (2)
O(23)	0.6229 (7)	0.1457 (5)	0.2892 (5)	6.7 (2)
O(31)	0.0170 (6)	0.3525 (3)	0.5872 (4)	3.5 (1)
O(32)	−0.1681 (6)	0.1531 (4)	0.5722 (5)	5.0 (2)
O(33)	−0.1941 (6)	0.2777 (4)	0.3388 (5)	5.3 (2)
O(42)	0.3734 (6)	0.2150 (3)	0.2242 (4)	4.0 (1)
O(43)	0.0491 (6)	0.2579 (3)	0.2412 (4)	3.9 (1)
O(51)	0.1706 (6)	0.0192 (3)	0.5467 (4)	4.0 (1)
C(11)	0.2939 (7)	0.2674 (4)	0.6173 (5)	2.6 (2)
C(12)	0.1313 (8)	0.1609 (5)	0.6403 (5)	3.2 (2)
C(13)	0.3698 (8)	0.1325 (5)	0.6293 (6)	3.5 (2)
C(21)	0.5348 (8)	0.0986 (5)	0.5025 (7)	4.1 (2)
(C22)	0.5482 (8)	0.2385 (5)	0.4966 (6)	3.2 (2)
C(23)	0.5556 (8)	0.1549 (5)	0.3443 (6)	3.9 (2)
C(31)	0.0202 (7)	0.3070 (5)	0.5395 (5)	2.9 (2)
C(32)	−0.0946 (8)	0.1813 (4)	0.5334 (6)	3.1 (2)
C(33)	−0.1130 (8)	0.2581 (5)	0.3849 (6)	3.2 (2)
C(42)	0.3384 (8)	0.2260 (4)	0.2950 (6)	3.1 (2)
C(43)	0.1152 (8)	0.2562 (4)	0.3077 (5)	2.9 (2)
C(44)	0.2444 (8)	0.3828 (4)	0.4592 (6)	3.1 (2)
C(45)	0.3709 (8)	0.3644 (4)	0.4639 (6)	3.1 (2)
C(46)	0.4057 (9)	0.3553 (5)	0.3738 (6)	3.6 (2)
C(47)	0.304 (1)	0.3671 (4)	0.3146 (6)	4.1 (2)
C(48)	0.202 (1)	0.3842 (4)	0.3656 (7)	4.4 (2)
C(51)	0.1832 (7)	0.0644 (4)	0.4966 (5)	2.4 (1)
C(52)	0.1947 (9)	0.0174 (4)	0.3186 (6)	4.0 (2)
C(53)	0.0682 (8)	0.0348 (4)	0.3243 (5)	3.3 (2)
C(54)	0.0455 (8)	0.0928 (4)	0.2685 (6)	3.6 (2)
C(55)	0.153 (1)	0.1087 (5)	0.2270 (5)	4.1 (2)
C(56)	0.2476 (9)	0.0624 (5)	0.2594 (6)	4.3 (2)
C(1)	0.348 (1)	0.0111 (5)	0.8490 (7)	4.8 (2)
C(2)	0.3768 (9)	0.0407 (6)	0.9332 (7)	5.2 (2)
C(3)	0.286 (1)	0.0574 (6)	0.9905 (7)	5.2 (3)
C(4)	0.1643 (9)	0.0439 (5)	0.9630 (8)	4.8 (2)
C(5)	0.137 (1)	0.0169 (6)	0.8794 (8)	5.9 (3)
C(6)	0.227 (1)	−0.0001 (6)	0.8229 (7)	5.7 (3)
H(1)	0.4133	−0.0017	0.8083	6.0
H(2)	0.4616	0.0495	0.9536	6.0
H(3)	0.3072	0.0785	1.0494	6.0
H(4)	0.0972	0.0533	1.0038	6.0
H(5)	0.0487	0.0101	0.8596	6.0
H(6)	0.2036	−0.0201	0.7639	6.0
H(44)	0.1955	0.3930	0.5102	5.0
H(45)	0.4250	0.3588	0.5189	5.0
H(46)	0.4879	0.3430	0.3566	5.0
H(47)	0.3037	0.3637	0.2487	5.0
H(48)	0.1174	0.3943	0.3404	5.0
H(52)	0.2381	−0.0198	0.3502	5.0
H(53)	0.0081	0.0116	0.3597	5.0
H(54)	−0.0329	0.1172	0.2606	5.0
H(55)	0.1625	0.1453	0.1838	5.0
H(56)	0.3339	0.0620	0.2432	5.0

[a] Anisotropic thermal parameters are given in supplementary material.

was phased on the metal atoms. Coordinates of hydrogens in the cyclopentadienyl rings were calculated with d(C–H) = 0.95 Å and B(H) = 5.5 Å². Full-matrix least-squares refinement were carried out by using anisotropic thermal parameters for non-hydrogen atoms. Final atomic positional parameters for compounds I and II are given in Tables III and IV, respectively.

Results and Discussion

In toluene at 90 °C, neither $[(\eta^5\text{-}C_5H_5)Mo(CO)_3]_2$ nor

Table IV. Atomic Coordinates and Isotropic Thermal Parameters of $(\mu\text{-}H)_3(\eta^5\text{-}C_5H_5)MoOs_3(CO)_{11}$[a] (Esd's in Parentheses)

atom	x	y	z	B, Å²
Os(11)	0.49390 (3)	0.19862 (4)	0.82202 (3)	2.35 (1)
Os(12)	0.55412 (3)	0.28260 (4)	0.97032 (3)	2.41 (1)
Os(13)	0.60909 (3)	0.34430 (4)	0.83825 (3)	2.73 (1)
Mo(14)	0.67380 (7)	0.17118 (8)	0.91275 (6)	2.32 (2)
C(11)	0.776 (1)	0.118 (1)	1.0135 (9)	5.3 (4)
C(12)	0.783 (1)	0.072 (1)	0.9481 (9)	4.9 (4)
C(13)	0.710 (1)	0.020 (1)	0.9230 (8)	4.5 (4)
C(14)	0.6594 (9)	0.035 (1)	0.9753 (8)	4.6 (3)
C(15)	0.6979 (9)	0.096 (1)	1.0298 (7)	4.0 (3)
C(111)	0.4014 (9)	0.2712 (9)	0.7699 (7)	3.1 (3)
O(111)	0.3434 (7)	0.3084 (8)	0.7363 (6)	5.1 (3)
C(112)	0.5185 (9)	0.166 (1)	0.7278 (8)	3.5 (3)
O(112)	0.5361 (8)	0.1475 (9)	0.6737 (5)	6.1 (3)
C(113)	0.4290 (8)	0.095 (1)	0.8316 (8)	3.6 (3)
O(113)	0.3901 (7)	0.0313 (8)	0.8389 (6)	5.2 (3)
C(121)	0.4780 (9)	0.365 (1)	1.0021 (7)	4.0 (3)
O(121)	0.4327 (8)	0.4116 (9)	1.0218 (6)	7.3 (3)
C(122)	0.6513 (9)	0.3215 (9)	1.0450 (7)	3.6 (3)
O(122)	0.7080 (7)	0.3431 (8)	1.0878 (6)	5.4 (3)
C(123)	0.5301 (9)	0.184 (1)	1.0292 (7)	3.5 (3)
O(123)	0.5110 (6)	0.1281 (9)	1.0644 (6)	5.4 (3)
C(131)	0.5209 (9)	0.414 (1)	0.7823 (8)	3.9 (3)
O(131)	0.4671 (7)	0.4570 (7)	0.7444 (6)	5.6 (3)
C(132)	0.647 (1)	0.325 (1)	0.7503 (7)	3.7 (3)
O(132)	0.6742 (7)	0.3184 (8)	0.6982 (5)	5.7 (3)
C(133)	0.6796 (9)	0.448 (1)	0.8707 (8)	4.2 (4)
O(133)	0.7144 (8)	0.5093 (9)	0.8916 (8)	7.6 (4)
C(141)	0.7049 (9)	0.152 (1)	0.8157 (7)	3.4 (3)
O(141)	0.7310 (7)	0.1325 (9)	0.7635 (5)	5.7 (3)
C(142)	0.7487 (8)	0.277 (1)	0.9280 (9)	3.9 (3)
O(142)	0.8066 (7)	0.3216 (9)	0.9472 (7)	6.4 (3)
Os(21)	0.11877 (4)	0.32742 (4)	0.96167 (3)	2.97 (1)
Os(22)	0.18064 (3)	0.39653 (4)	0.83392 (2)	2.57 (1)
Os(23)	0.16806 (3)	0.20102 (4)	0.86334 (3)	2.62 (1)
Mo(24)	0.01820 (7)	0.30836 (8)	0.79893 (6)	2.32 (2)
C(21)	−0.0555 (9)	0.368 (1)	0.6844 (8)	4.2 (3)
C(22)	−0.1103 (9)	0.317 (1)	0.7174 (9)	4.3 (4)
C(23)	−0.115 (1)	0.365 (1)	0.783 (1)	5.5 (4)
C(24)	−0.0605 (9)	0.444 (1)	0.7907 (9)	4.5 (4)
C(25)	−0.025 (1)	0.443 (1)	0.7279 (8)	4.3 (4)
C(211)	0.209 (1)	0.293 (1)	1.0403 (9)	5.3 (4)
O(211)	0.2628 (9)	0.275 (1)	1.0902 (7)	8.0 (4)
C(212)	0.047 (1)	0.252 (1)	0.9991 (8)	5.6 (4)
O(212)	0.0020 (9)	0.203 (1)	1.0191 (7)	7.5 (4)
C(213)	0.099 (1)	0.434 (1)	1.0145 (7)	4.5 (4)
O(213)	0.0852 (8)	0.496 (1)	1.0445 (7)	7.6 (4)
C(221)	0.2943 (8)	0.440 (1)	0.8570 (8)	3.1 (3)
O(221)	0.3591 (6)	0.4670 (8)	0.8658 (6)	4.9 (3)
C(222)	0.166 (1)	0.402 (1)	0.7285 (8)	4.2 (3)
O(222)	0.1587 (7)	0.4046 (9)	0.6632 (6)	5.7 (3)
C(223)	0.1371 (9)	0.516 (1)	0.8398 (8)	3.8 (3)
O(223)	0.1098 (8)	0.5873 (8)	0.8410 (8)	6.0 (3)
C(231)	0.2692 (9)	0.1839 (9)	0.9304 (8)	3.5 (3)
O(231)	0.3342 (7)	0.1755 (8)	0.9724 (6)	5.0 (3)
C(232)	0.1169 (9)	0.104 (1)	0.9092 (9)	4.1 (4)
O(232)	0.0886 (8)	0.0468 (7)	0.9372 (7)	5.7 (3)
C(233)	0.1995 (9)	0.126 (1)	0.7897 (9)	4.4 (4)
O(233)	0.2191 (7)	0.0814 (9)	0.7453 (7)	6.7 (3)
C(241)	−0.0327 (9)	0.195 (1)	0.8312 (8)	3.6 (3)
O(241)	−0.0686 (7)	0.1333 (8)	0.8452 (6)	5.1 (3)
C(242)	0.0612 (9)	0.229 (1)	0.7269 (7)	3.4 (3)
O(242)	0.0696 (7)	0.1897 (8)	0.6771 (6)	5.2 (3)
H(11)	0.8196	0.1617	1.0442	5.5
H(12)	0.8313	0.0752	0.9219	5.5
H(13)	0.6965	−0.0196	0.8756	5.5
H(14)	0.6027	0.0044	0.9724	5.5
H(15)	0.6748	0.1197	1.0730	5.5
H(21)	−0.0405	0.3513	0.6347	5.5
H(22)	−0.1401	0.2574	0.6984	5.5
H(23)	−0.1508	0.3478	0.8191	5.5
H(24)	−0.0504	0.4911	0.8336	5.5
H(25)	0.0165	0.4907	0.7166	5.5

[a] Anisotropic thermal parameters are given in supplementary material.

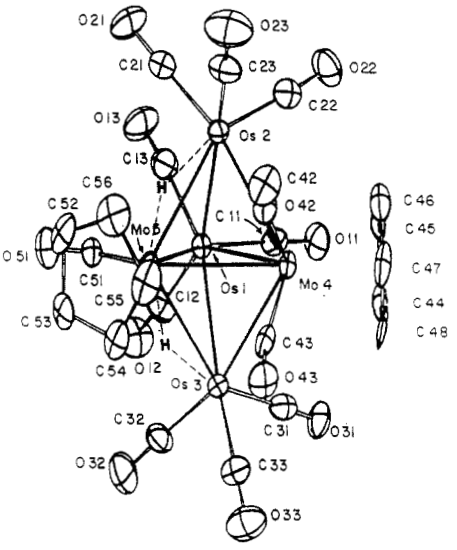

Figure 1. Structure of $(\mu\text{-H})_2(\eta^5\text{-}C_5H_5)_2Mo_2Os_3(CO)_{12}$.

Table V. Selected Interatomic Distances (Å) of $(\mu\text{-H})_2(\eta^5\text{-}C_5H_5)_2Mo_2Os_3(CO)_{12}\cdot C_6H_6$ (Esd's in Parentheses)

(A) Metal–Metal Distances			
Os(1)–Os(2)	2.844 (1)	Os(2)–Mo(4)	2.896 (1)
Os(1)–Os(3)	2.834 (1)	Os(2)–Mo(5)	2.999 (1)
Os(1)–Mo(4)	2.904 (1)	Os(3)–Mo(4)	2.908 (1)
Os(1)–Mo(5)	2.830 (1)	Os(3)–Mo(5)	3.015 (1)
		Mo(4)–Mo(5)	3.028 (1)
(B) Metal–C_5H_5 and Carbon–Carbon of C_5H_5 Distances			
Mo(4)–C(44)	2.403 (7)	Mo(5)–C(52)	2.263 (7)
Mo(4)–C(45)	2.395 (7)	Mo(5)–C(53)	2.279 (7)
Mo(4)–C(46)	2.340 (8)	Mo(5)–C(54)	2.323 (7)
Mo(4)–C(47)	2.312 (8)	Mo(5)–C(55)	2.388 (7)
Mo(4)–C(48)	2.343 (8)	Mo(5)–C(56)	2.331 (8)
C(44)–C(45)	1.402 (10)	C(52)–C(53)	1.407 (12)
C(45)–C(46)	1.413 (10)	C(53)–C(54)	1.416 (11)
C(46)–C(47)	1.373 (11)	C(54)–C(55)	1.377 (12)
C(47)–C(48)	1.404 (12)	C(55)–C(56)	1.420 (12)
C(48)–C(44)	1.425 (11)	C(56)–C(52)	1.386 (12)
(C) Metal–Carbonyl Distances			
Os(1)–C(11)	1.889 (8)	Os(3)–C(31)	1.914 (8)
Os(1)–C(12)	1.887 (8)	Os(3)–C(32)	1.888 (8)
Os(1)–C(13)	1.927 (8)	Os(3)–C(33)	1.906 (7)
Os(1)–C(51)	2.609 (7)	Os(3)–C(43)	2.640 (7)
Os(2)–C(21)	1.873 (9)	Mo(4)–C(42)	1.967 (8)
Os(2)–C(22)	1.896 (8)	Mo(4)–C(43)	1.957 (7)
Os(2)–C(23)	1.893 (8)	Mo(5)–C(51)	1.946 (7)
Os(2)–C(42)	2.620 (7)		
(D) Carbon–Oxygen Distances			
C(11)–O(11)	1.147 (8)	C(31)–O(31)	1.137 (9)
C(12)–O(12)	1.156 (9)	C(32)–O(32)	1.145 (9)
C(13)–O(13)	1.131 (9)	C(33)–O(33)	1.137 (8)
C(21)–O(21)	1.169 (10)	C(42)–O(42)	1.151 (9)
C(22)–O(22)	1.157 (9)	C(42)–O(43)	1.173 (8)

$[(\eta^5\text{-}C_5H_5)Mo(CO)_2]_2$ appear to react with $(\mu\text{-H})_2Os_3(CO)_{10}$ which is in accord with an earlier report.[7] However, when H_2 (1 atm) is present, clusters I, II, and III form (reaction 1). Yields of products appear to be a function of the

$$(\mu\text{-H})_2Os_3(CO)_{10} + [(\eta^5\text{-}C_5H_5)Mo(CO)_n]_2 \xrightarrow[\text{toluene/90 °C}]{H_2} \underset{n = 2,\ 3}{\text{I + II + III}} \quad (1)$$

effective H_2 concentration. Note in Table I that the pentanuclear cluster is the predominant product from both the saturated and unsaturated molybdenum dimers when an atmosphere of H_2 is placed over the stirred reaction mixture. However, when the effective hydrogen concentration is increased by bubbling H_2 through the reaction mixture, the yields of I diminished and those of II increased. Moreover, when the reaction was carried out under 9 atm of H_2, compound II was essentially the only product isolated. Furthermore, it was shown that compound I decomposes in the presence of H_2 at 90 °C, thereby not only accounting for diminished yields of I with increased H_2 concentration but also implying that I and II are formed through independent routes. The low yields of III probably arise from the conversion of III to II under reaction conditions.

Since a number of triosmium mixed-metal clusters have been prepared[3] from $(\mu\text{-H})_2Os_3(CO)_{10}$ under similar conditions of temperature and reaction time as clusters I–III, but in the absence of added H_2 we assume that the initial

Table VI. Selected Bond Angles (deg) of $(\mu\text{-H})_2(\eta^5\text{-}C_5H_5)Mo_2Os_3(CO)_{12}\cdot C_6H_6$ (Esd's in Parentheses)

(A) Angles within Mo_2Os_3 Pentanuclear Cluster			
Os(2)–Os(1)–Os(3)	113.56 (1)	Os(1)–Mo(4)–Os(2)	58.73 (1)
Os(2)–Os(1)–Mo(4)	60.50 (1)	Os(1)–Mo(4)–Os(3)	58.37 (1)
Os(2)–Os(1)–Mo(5)	63.81 (1)	Os(1)–Mo(4)–Mo(5)	56.95 (1)
Os(3)–Os(1)–Mo(4)	60.88 (1)	Os(2)–Mo(4)–Os(3)	109.86 (2)
Os(3)–Os(1)–Mo(5)	64.34 (1)	Os(2)–Mo(4)–Mo(5)	60.78 (2)
Mo(4)–Os(1)–Mo(5)	63.73 (2)	Os(3)–Mo(4)–Mo(5)	61.03 (2)
Os(1)–Os(2)–Mo(4)	60.77 (1)	Os(1)–Mo(5)–Os(2)	58.32 (1)
Os(1)–Os(2)–Mo(5)	57.87 (1)	Os(1)–Mo(5)–Os(3)	57.90 (1)
Mo(4)–Os(2)–Mo(5)	61.78 (2)	Os(1)–Mo(5)–Mo(4)	59.32 (1)
Os(1)–Os(3)–Mo(4)	60.75 (1)	Os(2)–Mo(5)–Os(3)	104.33 (2)
Os(1)–Os(3)–Mo(5)	57.77 (1)	Os(2)–Mo(5)–Mo(4)	57.44 (2)
Mo(4)–Os(3)–Mo(5)	61.45 (2)	Os(3)–Mo(5)–Mo(4)	57.52 (2)
(B) Metal–Metal–Carbon Angles			
Mo(4)–Os(3)–C(31)	90.4 (2)	Os(2)–Os(1)–C(11)	101.9 (2)
Mo(4)–Os(3)–C(32)	161.2 (2)	Os(2)–Os(1)–C(12)	158.3 (3)
Mo(4)–Os(3)–C(33)	109.6 (2)	Os(2)–Os(1)–C(13)	76.9 (2)
Os(1)–Os(3)–C(31)	90.1 (2)	Mo(4)–Os(1)–C(11)	83.1 (2)
Os(1)–Os(3)–C(32)	100.7 (2)	Mo(4)–Os(1)–C(12)	137.4 (2)
Os(1)–Os(3)–C(33)	169.8 (2)	Mo(4)–Os(1)–C(13)	135.1 (2)
Mo(5)–Os(3)–C(31)	144.2 (2)	Mo(5)–Os(1)–C(11)	146.8 (2)
Mo(5)–Os(3)–C(32)	107.5 (3)	Mo(5)–Os(1)–C(12)	109.5 (2)
Mo(5)–Os(3)–C(33)	115.7 (2)	Mo(5)–Os(1)–C(13)	111.0 (3)
Mo(4)–Os(2)–C(21)	159.5 (3)	Os(1)–Mo(4)–C(42)	113.6 (2)
Mo(4)–Os(2)–C(22)	88.8 (2)	Os(1)–Mo(4)–C(43)	113.4 (2)
Mo(4)–Os(2)–C(23)	112.8 (3)	Mo(5)–Mo(4)–C(42)	70.3 (2)
Os(1)–Os(2)–C(21)	98.7 (3)	Mo(5)–Mo(4)–C(43)	70.2 (2)
Os(1)–Os(2)–C(22)	94.4 (2)	Os(2)–Mo(4)–C(42)	61.8 (2)
Os(1)–Os(2)–C(23)	168.9 (2)	Os(2)–Mo(4)–C(43)	124.3 (2)
Mo(5)–Os(2)–C(21)	108.5 (2)	Os(3)–Mo(4)–C(42)	124.9 (2)
Mo(5)–Os(2)–C(22)	146.2 (2)	Os(3)–Mo(4)–C(43)	62.2 (2)
Mo(5)–Os(2)–C(23)	111.4 (2)	Os(1)–Mo(5)–C(51)	63.1 (2)
Os(3)–Os(1)–C(11)	99.4 (2)	Mo(4)–Mo(5)–C(51)	122.4 (2)
Os(3)–Os(1)–C(12)	78.1 (2)	Os(2)–Mo(5)–C(51)	92.5 (2)
Os(3)–Os(1)–C(13)	161.4 (2)	Os(3)–Mo(5)–C(51)	91.9 (2)
(C) Carbon–Metal–Carbon Angles			
C(11)–Os(1)–C(12)	93.7 (3)	C(22)–Os(2)–C(23)	94.5 (3)
C(11)–Os(1)–C(13)	93.0 (3)	C(31)–Os(3)–C(32)	92.7 (3)
C(12)–Os(1)–C(13)	87.4 (3)	C(31)–Os(3)–C(33)	93.5 (3)
C(21)–Os(2)–C(22)	93.5 (3)	C(32)–Os(3)–C(33)	88.7 (3)
C(21)–Os(2)–C(23)	87.4 (4)	C(42)–Mo(4)–C(43)	78.6 (3)
(D) Metal–Carbon–Oxygen Angles			
Os(1)–C(11)–O(11)	177.5 (7)	Os(3)–C(33)–O(33)	178.4 (7)
Os(1)–C(12)–O(12)	174.3 (7)	Mo(4)–C(42)–O(42)	161.9 (7)
Os(1)–C(13)–O(13)	170.6 (7)	Mo(4)–C(43)–O(43)	162.4 (6)
Os(2)–C(21)–O(21)	178.9 (8)	Os(2)–C(42)–O(42)	120.1 (6)
Os(2)–C(22)–O(22)	176.6 (7)	Os(3)–C(43)–O(43)	119.7 (6)
Os(2)–C(23)–O(23)	177.7 (8)	Mo(5)–C(51)–O(51)	163.8 (6)
Os(3)–C(31)–O(31)	176.7 (7)	Os(1)–C(51)–O(51)	120.9 (5)
Os(3)–C(32)–O(32)	177.4 (7)		
(E) Angles within η^5-C_5H_5 Ring			
C(44)–C(45)–C(46)	107.4 (7)	C(52)–C(53)–C(54)	106.8 (8)
C(45)–C(46)–C(47)	109.2 (7)	C(53)–C(54)–C(55)	108.8 (8)
C(46)–C(47)–C(48)	108.2 (7)	C(54)–C(55)–C(56)	107.9 (8)
C(47)–C(48)–C(44)	107.8 (8)	C(55)–C(56)–C(52)	107.8 (8)
C(48)–C(44)–C(45)	107.3 (7)	C(56)–C(52)–C(53)	108.7 (7)

Since a number of triosmium mixed-metal clusters have been prepared[3] from $(\mu\text{-H})_2Os_3(CO)_{10}$ under similar conditions of temperature and reaction time as clusters I–III, but in the absence of added H_2 we assume that the initial

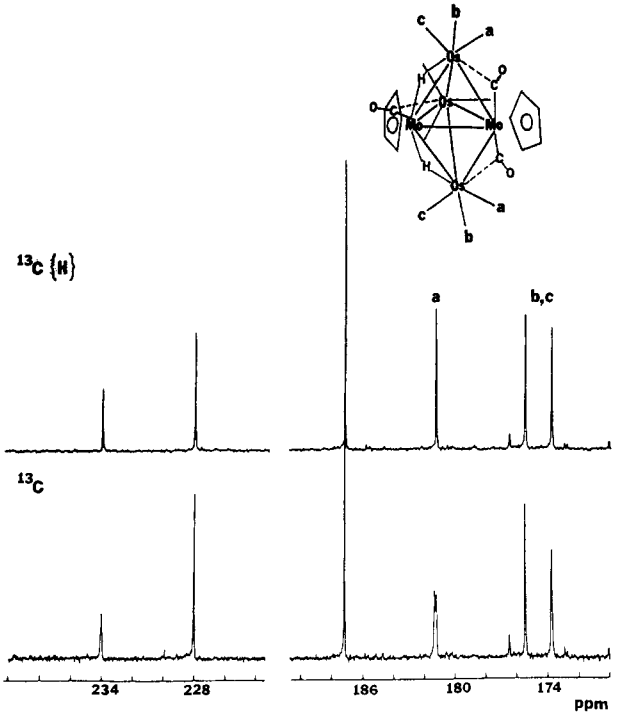

Figure 2. Carbon-13 NMR spectra of $(\mu\text{-H})_2(\eta^5\text{-}C_5H_5)_2Mo_2Os_3(CO)_{12}$.

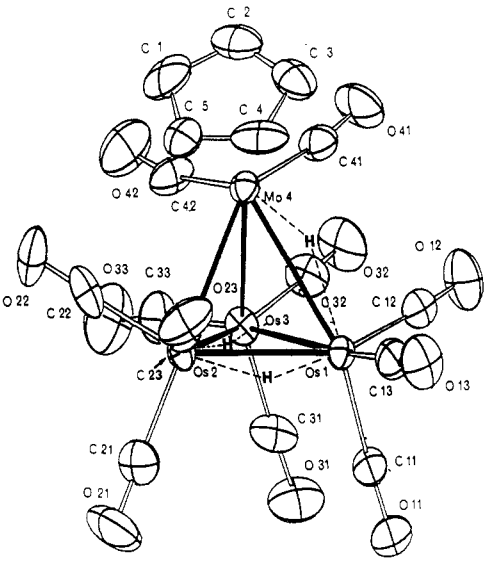

Figure 3. Structure of $(\mu\text{-H})_3(\eta^5\text{-}C_5H_5)MoOs_3(CO)_{11}$.

step in the presence of dihydrogen is the formation on an intermediate hydride.[26] A likely possibility is a dimolybdenum hydride formed from the unsaturated molybdenum dimer. Under the reaction conditions chosen, when the saturated molybdenum dimer is the starting material, it slowly converts to the unsaturated dimer. A reasonable choice for dimolybdenum hydride is $[(\eta^5\text{-}C_5H_5)MoH_2(CO)_2]_2$, a hydride for which there is evidence as a transient species.[7] Such a species might react with $(\mu\text{-H})_2Os_3(CO)_{10}$ to give the pentanuclear cluster I. That cluster II is favored at high effective H_2 concentration and that I and II appear to form independently of each other suggest to us that when the effective H_2 concentration is increased, a mononuclear molybdenum hydride is favored over a dinuclear species. The mononuclear hydride might react with $(\mu\text{-H})_2Os_3(CO)_{10}$ to give rise to the tetranuclear clusters II and III.

Table VII. Selected Interatomic Distances (Å) of $(\mu\text{-H})_3(\eta^5\text{-}C_5H_5)MoOs_3(CO)_{11}$ (Esd's in Parentheses)

	molecule 1	molecule 2
(A) Metal–Metal Distances		
Os(1)–Os(2)	2.938 (1)	2.933 (1)
Os(1)–Os(3)	2.825 (1)	2.821 (1)
Os(1)–Mo(4)	3.092 (1)	3.079 (1)
Os(2)–Os(3)	2.909 (1)	2.916 (1)
Os(2)–Mo(4)	2.935 (1)	2.919 (1)
Os(3)–Mo(4)	2.952 (1)	2.946 (1)
(B) Metal–Carbon Distances		
Os(1)–C(11)	1.93 (1)	1.88 (2)
Os(1)–C(12)	1.92 (1)	1.85 (1)
Os(1)–C(13)	1.89 (1)	1.91 (1)
Os(2)–C(21)	1.92 (1)	1.94 (1)
Os(2)–C(22)	1.95 (1)	1.90 (1)
Os(2)–C(23)	1.90 (1)	1.90 (1)
Os(3)–C(31)	1.88 (1)	1.85 (1)
Os(3)–C(32)	1.87 (1)	1.92 (1)
Os(3)–C(33)	1.92 (1)	1.90 (1)
Os(3)–C(42)	2.70 (1)	2.75 (1)
Mo(4)–C(41)	1.98 (1)	2.00 (1)
Mo(4)–C(42)	1.96 (1)	2.00 (1)
(C) Distances Involving the $\eta^5\text{-}C_5H_5$ Ligand		
Mo(4)–C(1)	2.34 (1)	2.35 (1)
Mo(4)–C(2)	2.30 (1)	2.32 (1)
Mo(4)–C(3)	2.28 (1)	2.32 (1)
Mo(4)–C(4)	2.33 (1)	2.37 (1)
Mo(4)–C(5)	2.36 (1)	2.39 (1)
C(1)–C(2)	1.40 (2)	1.41 (2)
C(2)–C(3)	1.41 (2)	1.40 (2)
C(3)–C(4)	1.43 (2)	1.45 (2)
C(4)–C(5)	1.38 (2)	1.41 (2)
C(5)–C(1)	1.43 (2)	1.39 (2)
(D) Carbon–Oxygen Distances		
C(11)–O(11)	1.15 (1)	1.16 (2)
C(12)–O(12)	1.13 (1)	1.16 (2)
C(13)–O(13)	1.16 (1)	1.10 (1)
C(21)–O(21)	1.13 (1)	1.12 (1)
C(22)–O(22)	1.12 (2)	1.17 (1)
C(23)–O(23)	1.13 (1)	1.14 (1)
C(31)–O(31)	1.17 (2)	1.18 (1)
C(32)–O(32)	1.15 (1)	1.14 (2)
C(33)–O(33)	1.10 (2)	1.15 (1)
C(41)–O(41)	1.17 (1)	1.14 (1)
C(42)–O(42)	1.14 (1)	1.11 (1)

$(\mu\text{-H})_2(\eta^5\text{-}C_5H_2)_2Mo_2Os_3(CO)_{12}$. A single crystal of the benzene solvate of I, $(\mu\text{-H})_2(\eta^5\text{-}C_5H_5)_2Mo_2Os_3(CO)_{12}\cdot C_6H_6$, was obtained at −15 °C, and the molecular structure was determined (Figure 1) from an X-ray study. Selected bond distances and bond angles are listed in Tables V and VI. The metal framework of I is a trigonal bipyramid in which two molybdenum atoms and one osmium atom occupy the equatorial vertices. Three terminal carbonyls are bound to each osmium atom while Mo(5) is bound to a carbonyl semibridging to Os(1), and Mo(4) is bound to two carbonyls semibridging to Os(2) and Os(3). A cyclopentadienyl group is bound to each molybdenum. Hydrogen bridges Os(2)–H–Mo(5) and Os(3)–H–Mo(5) are inferred from structural and NMR data. Formation of the cluster might be visualized as insertion of a molybdenum dimer normal to an edge of the Os_3 triangle of $(\mu\text{-H})_2Os_3(CO)_{10}$, thereby causing two osmium atoms to move to the apical vertices of the resulting trigonal bipyramid. The molecule has approximate C_s symmetry with the mirror plane being defined by the least-squares plane Os(1), Mo(4), Mo(5), C(11), O(11), C(47), and C(55). Deviations from this plane range from 0.064 to −0.054 Å.

The metal framework of I is associated with 72 valence electrons, and the formal electron counts at the metal atoms, not taking into account possible contributions from

Table VIII. Selected Bond Angles (deg) of $(\mu\text{-H})_3(\eta^5\text{-}C_5H_5)MoOs_3(CO)_{11}$ (Esd's in Parentheses)

	molecule 1	molecule 2
(A) Angles within Os_3Mo Tetrahedral Cluster		
Os(2)–Os(1)–Os(3)	60.60 (1)	60.88 (1)
Os(2)–Os(1)–Mo(4)	58.12 (2)	58.04 (2)
Os(3)–Os(1)–Mo(4)	59.66 (2)	59.71 (2)
Os(1)–Os(2)–Os(3)	57.77 (1)	57.66 (1)
Os(1)–Os(2)–Mo(4)	63.53 (2)	63.49 (2)
Os(3)–Os(2)–Mo(4)	60.68 (2)	60.63 (2)
Os(1)–Os(3)–Os(2)	61.63 (1)	61.46 (1)
Os(1)–Os(3)–Mo(4)	64.67 (2)	64.51 (2)
Os(2)–Os(3)–Mo(4)	60.09 (2)	59.73 (2)
Os(1)–Mo(4)–Os(2)	58.29 (2)	58.47 (2)
Os(1)–Mo(4)–Os(3)	55.67 (2)	55.78 (2)
Os(2)–Mo(4)–Os(3)	59.23 (2)	59.64 (2)
(B) Metal–Metal–Carbon Angles		
Os(2)–Os(1)–C(11)	107.0 (3)	109.7 (5)
Os(2)–Os(1)–C(12)	146.6 (4)	149.7 (4)
Os(2)–Os(1)–C(13)	109.3 (4)	104.6 (4)
Os(3)–Os(1)–C(11)	94.6 (3)	90.9 (4)
Os(3)–Os(1)–C(12)	90.2 (4)	98.5 (5)
Os(3)–Os(1)–C(13)	168.2 (4)	165.3 (4)
Mo(4)–Os(1)–C(11)	153.9 (4)	150.6 (4)
Mo(4)–Os(1)–C(12)	94.3 (4)	93.0 (4)
Mo(4)–Os(1)–C(13)	110.3 (4)	116.3 (4)
Os(1)–Os(2)–C(21)	115.4 (4)	115.6 (3)
Os(1)–Os(2)–C(22)	145.5 (3)	147.2 (4)
Os(1)–Os(2)–C(23)	97.9 (4)	93.7 (4)
Os(3)–Os(2)–C(21)	113.8 (4)	112.7 (4)
Os(3)–Os(2)–C(22)	97.4 (3)	103.4 (4)
Os(3)–Os(2)–C(23)	148.6 (4)	147.4 (4)
Mo(4)–Os(2)–C(21)	174.3 (4)	173.0 (4)
Mo(4)–Os(2)–C(22)	84.0 (3)	84.0 (4)
Mo(4)–Os(2)–C(23)	91.7 (4)	94.2 (4)
Os(1)–Os(3)–C(31)	85.8 (4)	90.8 (4)
Os(1)–Os(3)–C(32)	98.6 (4)	89.0 (4)
Os(1)–Os(3)–C(33)	166.8 (4)	173.4 (5)
Os(2)–Os(3)–C(31)	105.5 (3)	99.3 (3)
Os(2)–Os(3)–C(32)	153.5 (3)	148.3 (4)
Os(2)–Os(3)–C(33)	105.6 (4)	112.4 (4)
Mo(4)–Os(3)–C(31)	150.4 (4)	152.7 (4)
Mo(4)–Os(3)–C(32)	96.4 (3)	98.7 (4)
Mo(4)–Os(3)–C(33)	113.4 (4)	110.8 (4)
Os(1)–Mo(4)–C(41)	87.3 (2)	87.9 (4)
Os(1)–Mo(4)–C(42)	118.3 (4)	119.6 (3)
Os(2)–Mo(4)–C(41)	137.4 (3)	136.6 (4)
Os(2)–Mo(4)–C(47)	88.1 (4)	87.2 (4)
Os(3)–Mo(4)–C(41)	81.4 (3)	79.4 (4)
Os(3)–Mo(4)–C(42)	62.7 (4)	64.2 (3)
(C) Carbon–Metal–Carbon Angles		
C(11)–Os(1)–C(12)	90.0 (5)	91.3 (7)
C(11)–Os(1)C(13)	94.6 (5)	92.0 (6)
C(12)–Os(1)–C(13)	97.3 (5)	95.9 (6)
C(21)–Os(2)–C(22)	95.8 (5)	96.0 (5)
C(21)–Os(2)–C(23)	94.0 (5)	92.8 (5)
C(22)–Os(2)–C(23)	93.9 (5)	93.2 (5)
C(31)–Os(3)–C(32)	89.2 (5)	91.9 (5)
C(31)–Os(3)–C(33)	94.9 (6)	92.7 (5)
C(32)–Os(3)–C(33)	94.6 (5)	96.4 (6)
C(41)–Mo(4)–C(42)	87.5 (5)	87.2 (5)
(D) Metal–Carbon–Oxygen Angles		
Os(1)–C(11)–O(11)	174 (1)	176 (1)
Os(1)–C(12)–O(12)	177 (1)	177 (1)
Os(1)–C(13)–O(13)	178 (1)	178 (1)
Os(2)–C(21)–O(21)	178 (1)	175 (1)
Os(2)–C(22)–O(22)	179 (1)	179 (1)
Os(2)–C(23)–O(23)	175 (1)	178 (1)
Os(3)–C(31)–O(31)	176 (1)	178 (1)
Os(3)–C(32)–O(32)	175 (1)	178 (1)
Os(3)–C(33)–O(33)	174 (1)	179 (1)
Mo(4)–C(41)–O(41)	171 (1)	173 (1)
Mo(4)–C(42)–O(42)	161 (1)	165 (1)
(E) Angles within $\eta^5\text{-}C_5H_5$ Ring		
C(1)–C(2)–C(3)	108 (1)	105 (1)
C(2)–C(3)–C(4)	107 (1)	110 (1)
C(3)–C(4)–C(5)	109 (1)	106 (1)
C(4)–C(5)–C(1)	108 (1)	108 (1)
C(5)–C(1)–C(2)	108 (1)	111 (1)

the semibridging carbonyls, are as follows: Os(1), 18e; Os(2 and 3), $17^1/_2$ e; Mo(4), 19e; Mo(5), 18e. The carbonyls on Mo(4) are semibridging with respect to the apical osmium atoms and are believed to help balance charge between these formally electron-deficient Os atoms and the formally electron-rich Mo(4). However, this simple rationale for correlation of structure with charge distributions is inadequate for this particular heteronuclear cluster since it does not account for the existence of the semibridging carbonyl C(51)–O(51) between the formally electron-sufficient atoms Mo(5) and Os(1). Indeed, carbon–osmium distances [C(42)–Os(2) = 2.622 (8), C(43)–Os(3) = 2.647 (8), C(51)–Os(1) = 2.609 (7) Å] and ^{13}C NMR chemical shift data [$\delta_{C(42),C(43)}$ 228; $\delta_{C(51)}$ 234] suggest that the semibridging C(51) atom interacts more strongly with Os(1) than the semibridging carbons C(42) and C(43) interact with Os(2) and Os(3), respectively. Therefore, the lowest band, 1842 cm^{-1}, in the CO stretching region of the IR spectrum of I (see Experimental Section) is assigned to this semibridging carbonyl C(51)–O(51). Bond angles for the semibridging carbonyls are as follows: Mo(4)–C(42)–O(42) = 161.91 (7)°, Mo(4)–C(43)–O(43) = 162.4 (6)°, Mo(5)–C(51)–O(51) = 163.8 (6)°.

Although the positions of the two hydrogen atoms were not determined directly from the X-ray data, they are inferred as edge-bridging between Mo(5) and Os(2) and Mo(5) and Os(3). The distances Os(2)–Mo(5) = 2.999 (1) Å and Os(3)–Mo(5) = 3.015 (1) Å are significantly longer than the remaining molybdenum–osmium bonding distances in the molecule: Os(2)–Mo(4) = 2.896 (1) Å, Os(3)–Mo(4) = 2.908 (1) Å, Os(1)–Mo(4) = 2.904 (1) Å, Os(1)–Mo(5) = 2.830(1)Å. Additional support for this arrangement of hydrogen atoms in I comes from its ^1H NMR spectrum which is discussed below.

The distance Mo(4)–Mo(5) is 3.028 (1) Å compared to that in $[(\eta^5\text{-}C_5H_5)Mo(CO)_3]_2$ which is 3.235 (1) Å.[12] Osmium–osmium bond distances, Os(1)–Os(2) = 2.844 (1) Å, and Os(1)–Os(3) = 2.834 (1) Å, are consistent with those in $Os_3(CO)_{12}$, 2.8737 (5)–2.8824 (5) Å,[13] and in $(\eta^5\text{-}C_5H_5)RhOs_2(CO)_9$, 2.846 (1) Å.[3]

The dihedral angle between the C_5H_5 rings is 127.2°. The fivefold axis of each ring does not pass through the capping molybdenum atom. Mo–C distances are in the range 2.317 (8)–2.413 (8)Å for Mo(4)–$(\eta^5\text{-}C_5H_5)$ and 2.275

(12) Adams, R. D.; Collins, D. M.; Cotton, F. A. *Inorg. Chem.* **1974**, *13*, 1086.
(13) Churchill, M. R.; DeBoer, B. G. *Inorg. Chem.* **1977**, *16*, 878.

Figure 4. Proposed arrangements of bridging hydrogens in $(\mu\text{-H})_3(\eta^5\text{-}C_5H_5)MoOs_3(CO)_{11}$ and $(\mu\text{-H})_3(\eta^5\text{-}C_5H_5)WOs_3(CO)_{11}$.

(7)–2.395 (8)Å for Mo(5)–(η^5-C_5H_5). Such differences also occur in other cyclopentadienyl cluster complexes.[3,6,18] The distance between the center of a C_5H_5 ring to Mo(4) and to Mo(5) is 2.033 and 1.985 Å, respectively.

The proton NMR spectrum of I in $CDCl_3$ at 25 °C consists of three signals: 5.56 (s, 5 H), 4.90 (s, 5 H), and −18.2 ppm (s, 2 H). The two low-field resonances of relative area 5 arise from the nonequivalent C_5H_5 rings while the high-field signal of relative area 2 is assigned to the bridging hydrogens in equivalent environments, related by the mirror plane of the molecule.

The carbon-13 NMR spectrum of I in CH_2Cl_2 at 25 °C (Figure 2) consists of six signals which appear to be temperature invariant. This spectral pattern is consistent with the structure shown in the solid state. The two lowest field peaks are assigned to the semibridging carbonyls: the equivalent carbonyls across Mo(4)–Os(2) and Mo(4)–Os(3) (228.0 ppm, relative intensity 2) and the carbonyl across Mo(5)–Os(1) (234.0 ppm, relative intensity 1). The doublet at 181.3 ppm (relative area 2) is assigned to carbonyls **a** which are trans to a bridging H atom. The singlets at 175.4 and 173.7 ppm of relative intensities 2 are assigned to carbonyls **b** or **c**, but further distinction between them cannot be made. Finally the singlet of relative intensity 3 at 187.2 ppm is assigned to the carbonyls on the equatorial plane. Resolution of the expected signals in a 2:1 intensity ratio could not be achieved at −90 °C. This fluxional behavior is probably due to the facial rotation of the three carbonyls along the axis which passes through the equatorial osmium and the midpoint of the Mo–Mo bond.

Few heteropentanuclear metal clusters have been reported. Among these only $[M_2Ni_3(CO)_{16}]^{2-}$ (M = Mo, W),[14] $Pt_3Co_2(CO)_6[P(C_6H_5)_3]_3$,[15] and $[PtRh_4(CO)_{12}]^{2-}$[16] have a trigonal-bipyramidal structure with a Ni_3, a Co_2Pt, and a Rh_3 equatorial triangle, respectively.

$(\mu\text{-H})_3(\eta^5\text{-}C_5H_5)MoOs_3(CO)_{11}$. The structure of II was determined from a single-crystal X-ray study (Figure 3). Two independent molecules are in the asymmetric unit; they have the same gross structure. Selected bond distances and bond angles are listed in Tables VII and VIII, respectively. The metal framework of II consists of a tetrahedron. Three terminal carbonyls are bound to each osmium atom; Mo(4) is bound to a terminal carbonyl, a cyclopentadienyl group, and a semibridging carbonyl to Os(2). Hydrogen bridges Os(1)–H–Os(2), Os(2)–H–Os(3), and Os(1)–H–Mo(4) are inferred from structural and NMR data.

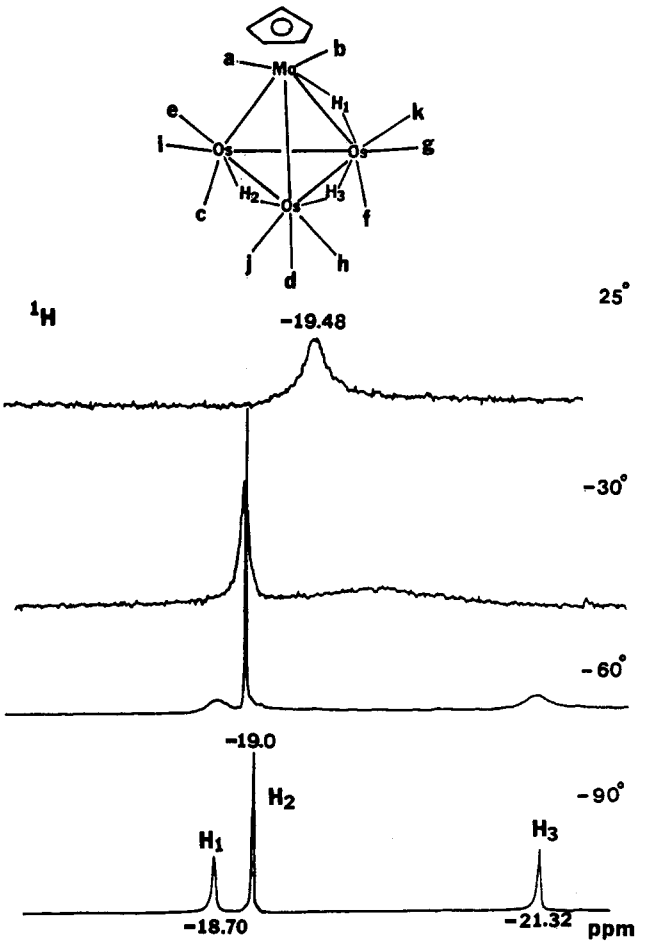

Figure 5. Proton NMR spectrum of $(\mu\text{-H})_3(\eta^5\text{-}C_5H_5)MoOs_3(CO)_{11}$.

The metal framework of cluster II is associated with 60 valence electrons, and the formal electron counts at the metal atoms, based on Figure 3 and not taking into account a possible contribution from the semibridging carbonyl, are as follows: Os(1), 18e; Os(2), 18e; Os(3), $17^1/_2$e; Mo(4), $18^1/_2$e. The semibridging carbonyl between Mo(4) and Os(3) probably helps to balance the charge between the formally electron-deficient Os atom and the formally electron-rich Mo atom. The average bond angle of this semibridging carbonyl in the two independent molecules is Mo(4)–C(42)–O(42) = 163 [2]°.[23] The average distance of the semibridging C(42) atom to Os(3) (2.733 [3] Å[23]) is longer than that for the semibridging carbons in I and the ^{13}C NMR shift (δ 222.6) occurs at higher field, thereby suggesting less interaction of this carbon with osmium than for the semibridging carbons in cluster I. In fact no low-frequency band in the carbonyl stretching region is observed in the infrared spectrum of II which can be assigned to the semibridging carbonyl as is observed in the case of I.

The positions of the three hydrogen atoms were not located directly from X-ray data. However, they are inferred as edge-bridging between Os(1)–Os(2), Os(2)–Os(3), and Mo(4)–Os(1), since the average of each of these distances in the two molecules, Os(1)–Os(2) = 2.936 [2] Å, Os(2)–Os(3) = 2.913 [3] Å, and Os(1)–Mo(4) = 3.086 [5] Å,[23] is significantly longer than the average value of each of the remaining osmium–osmium and osmium–molybdenum distances: Os(1)–Os(3) = 2.823 [2] Å, Os(2)–Mo(4)

(14) Ruff, J. K.; White, R. P., Jr.; Dahl, L. F. *J. Am. Chem. Soc.* **1971**, *93*, 2159.
(15) Barbier, J.-P.; Braunstein, P.; Fischer, J. and Ricard, L. *Inorg. Chim. Acta* **1978**, L361.
(16) Fumagalli, A.; Martinengo, S.; Chini, P.; Galli, D.; Heaton, B. T.; Pergola, R. D. *Inorg. Chem.* **1984**, *23*, 2947.
(17) Bhadmi, S.; Johnson, B. F. G.; Lewis, J.; Raithby, P. R.; Watson, D. J. *J. Chem. Soc., Chem. Commun.* **1978**, 343.
(18) Churchill, M. R.; Hollander, F. J. *Inorg. Chem.* **1979**, *18*, 843.
(19) Geoffroy, G. L.; Gladfelter, W. L. *Inorg. Chem.* **1980**, *19*, 2579.
(20) Knight, J.; Mays, M. J. *J. Chem. Soc., Dalton Trans.* **1972**, 1022.
(21) Churchill, M. R.; Hollander, F. J.; Lashewycz, R. A.; Pearson, G. A.; Shapley, J. R. *J. Am. Chem. Soc.* **1981**, *103*, 2430.
(22) Kennedy, S.; Alexander, J. J.; Shore, S. G. *J. Organomet. Chem.* **1981**, *219*, 385.
(23) The error estimate shown in brackets for the average distance was obtained from the expression $[\sum_{i=1}^{n}(d_i - \bar{d})^2/(n^2 - 1)]^{1/2}$.
(24) Todd, L. J.; Wilkinson, J. R. *J. Organomet. Chem.* **1974**, *77*, 1.

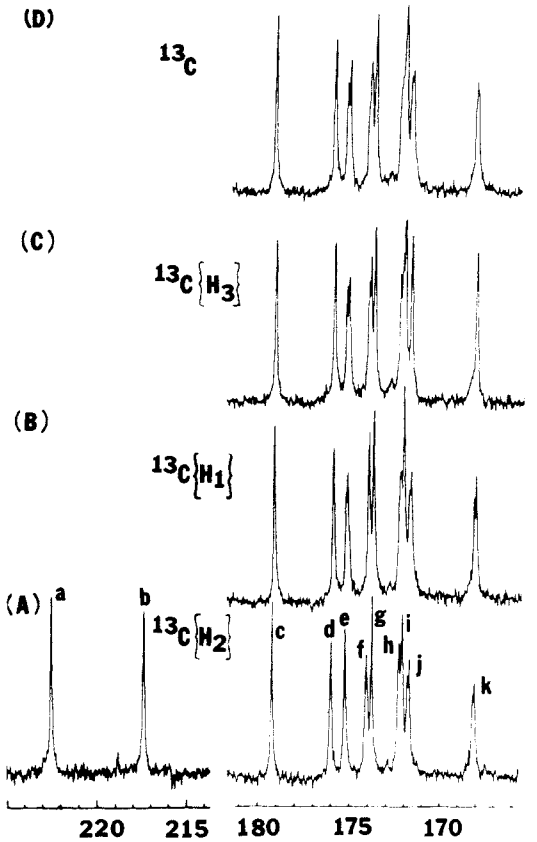

Figure 6. Carbon-13 NMR spectrum of $(\mu\text{-H})_3(\eta^5\text{-}C_5H_5)MoOs_3(CO)_{11}$.

= 2.927 [7] Å, Os(3)–Mo(4) = 2.949 [2] Å.[23] The longer osmium–osmium distances are comparable to distances reported for Os–H–Os bonds in the clusters $(\mu\text{-H})_2FeOs_3(CO)_{13}$,[2] $(\mu\text{-H})_3(\eta^5\text{-}C_5H_5)WOs_3(CO)_{11}$,[11] $(\mu\text{-H})_3CoOs_3(CO)_{13}$,[17] and $(\mu\text{-H})_2(\eta^5\text{-}C_5H_5)CoOs_3(CO)_{10}$.[6] Furthermore, the positions of bridging hydrogens in II, based on a comparison of metal–metal distances, are also supported by the ^1H NMR spectrum of II which is described below. The unbridged Os–Os distances are consistent with those similarly assigned in I and in previously reported reported clusters.[2,6] The Mo–Os distances in II assigned to hydrogen-bridged and non-hydrogen-bridged bonds are consistent with those assigned in I. Interestingly, the arrangement of hydrogen atoms in II is different from that in the isoelectronic analogue[11] $(\mu\text{-H})_3(\eta^5\text{-}C_5H_5)WOs_3(CO)_{11}$ in which there are two W–H–Os bonds and one Os–H–Os bond (Figure 4).

The dihedral angle between the $\eta^5\text{-}C_5H_5$ ring and the Os_3 plane is 32.1° in molecule 1 and 33.9° in molecule 2. The fivefold axis of the ring does not pass through the capping molybdenum atom. The cyclopentadiene C–Mo distances range from 2.28 (1) to 2.37 (1) Å in molecule 1 and from 2.32 (1) to 2.39 (1) Å in molecule 2. The distance between the center of the C_5H_5 ring and Mo(4) is 1.985 Å for molecule 1 and 2.006 Å for molecule 2.

The limiting proton NMR spectrum of II at −90 °C in CD_2Cl_2 is shown in Figure 5. In addition to a sharp singlet of relative intensity 5 at 5.30 ppm which is assigned to the cyclopentadienyl group, there are three distinct signals of relative intensity 1 at −18.7, −19.0, and −21.3 ppm which are in the region expected for edge-bridging hydrogens. The signals assigned to H_1 and H_3 broaden as the temperature is raised and coalesce at about −30 °C. At room temperature all three hydrogens exchange rapidly, resulting in a singlet at −19.5 ppm, while the cyclopentadienyl signal remains unchanged at all temperatures.

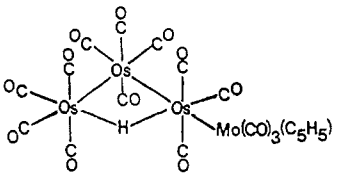

Figure 7. Proposed structure of $(\mu\text{-H})(\eta^5\text{-}C_5H_5)MoOs_3(CO)_{14}$.

The resonance at −18.7 ppm is assigned to H_1 due to the observation that a hydrogen atom bridging a heterometal and osmium generally has a resonance at lower field than hydrogen bridging two osmium atoms.[25] The signals at −21.3 and −19.0 ppm are assigned to H_3 and H_2, respectively, based on the ground that the Os(1)–Os(2) bond is more electron-abundant than the Os(2)–Os(3) bond based on electron counting.[11] The same phenomenon has also been observed in the proton NMR spectra of $(\mu\text{-H})_2(\eta^5\text{-}C_5H_5)MoOs_3(CO)_{10}$ (M = Rh, Co).[3,6] Confirmation of this distinction between H_2 and H_3 was made by means of selective proton decoupling of the ^{13}C NMR spectra.

The carbon-13 NMR spectrum at room temperature displays a broad peak of relative area 2 at 220.0 ppm which is assigned to the carbonyls on molybdenum and a broad peak of relative area 9 at 193.6 ppm which is assigned to the carbonyls on the osmium atoms. The lack of resolution in these signals is attributed to local rotation of the CO groups and hydrogen migration among the available metal–metal sites. Under the condition of slow exchange (−90 °C) and employing broad band proton decoupling, these two bands are resolved into two and nine bands, respectively, each with a relative area of 1 (Figure 6d). The appearance of eleven resonances at low temperature is consistent with the C_1 point symmetry of the molecular structure in the solid state. The lowest field peaks at 222.6 and 217.4 ppm are in the reported region for terminal carbonyls on molybdenum containing a cyclopentadienyl unit.[24] The resonance at 222.6 ppm is further assigned to the semibridging carbonyl a. This assignment is based on the unambiguous assignments made in the ^{13}C NMR spectrum of $(\mu\text{-H})_2FeOs_3(CO)_{13}$ in which the semibridging carbonyl resonance from Fe to Os is downfield from the resonances of the terminal carbonyls on iron.[2]

The signal at 174.0 ppm is assigned to axial carbonyl **f** which is trans to H_1 since it is the only doublet which collapses to a singlet in the $^{13}C\{H_1\}$ spectrum (Figure 6b). Also noteworthy in this spectrum is the doublet which appears at 168.1 ppm and can be assigned to the equatorial carbonyl **k** which is cis to H_1. The assignment of H_3 to the resonance at −21.3 ppm is confirmed by the collapse of the doublet of carbonyl **k** to a singlet in the $^{13}C\{H_3\}$ spectrum (Figure 6c). Also, the doublet at 171.7 ppm in the undecoupled spectrum collapses to a singlet in the $^{13}C\{H_3\}$ spectrum and is therefore assigned to the equatorial carbonyl **j** which is *trans* to H_3. The equatorial carbonyls **h**, 172.3 ppm (J = 9.6 Hz), and **e**, 175.3 ppm (J = 9.6 Hz), are trans to H_2 and are assigned on the basis of similar arguments. These signals are further distinguished by the observation that the signal assigned to **h** shows only partial collapse in the $^{13}C\{H_3\}$ NMR spectrum with residual coupling from H_2. On the other hand the signal assigned to **e** collapses to a clean singlet in the $^{13}C\{H_2\}$ NMR spectrum but is a doublet in the $^{13}C\{H_3\}$ spectrum. The signals at 179.3 and 176.0 ppm are assigned to the axial carbonyls **c** and **d** while the signals at 173.8 and 172.1 ppm are as-

(25) Robert, D. A.; Geoffrey, G. L. In *Comprehensive Organometallic Chemistry*; Stone, F. G. A., Abel, E. W., Eds.; Pergamon Press: Oxford, 1982; Vol. 6, pp 763–877.

signed to the equatorial carbonyls **g** and **i**. These assignments are based upon earlier observations that the resonances of axial carbonyls in this type of cluster occur at lower field than those of equatorial carbonyls.[2,19]

$(\mu$-H)$(\eta^5$-$C_5H_5)MoOs_3(CO)_{14}$. Compound III was characterized by its FT-ICR mass spectrum and its ^1H NMR spectrum. The mass spectrum showed a parent ion peak which corresponds to the molecular formula $^1H_6{}^{12}C_{19}{}^{16}O_{14}{}^{98}Mo^{192}Os_3$ (m/e(obsd) 1131.97; m/e(calcd) 1131.88). The loss of each of the first 13 carbonyls was visible in a single spectrum, and the Mo_2Os_3 stoichiometry was established from the relative intensities within each multiplet. The ^1H NMR spectrum in $CDCl_3$ at 28 °C consists of a singlet of relative intensity 5 at 5.28 ppm which is assigned to the cyclopentadienyl group and a singlet of relative intensity 1 at −20.51 ppm which is assigned to a bridge hydrogen. A proposed structure which satisfies the 18-electron rule is shown in Figure 7. The crystal structure of an isoelectronic analogue $(\mu$-H)$Os_3Re(CO)_{15}(NCCH_3)$[26] has been reported. Several other mixed-metal clusters, i.e., $HReOs_3(CO)_{16}$,[20,21] $H_2MnOs_3(CO)_{15}^{1-}$, and $H_2FeOs_3(CO)_{14}^{1-}$[22] have also been suggested to have the same type of structure.

Acknowledgment. We thank the National Science Foundation for support of this work through Grant CHE 84-11630. We thank Tao-Chin Lin Wang, Annjia T. Hsu, and Professor Alan G. Marshall for FT/ICR mass spectra and C. R. Weisenberger for high-resolution mass spectra. NMR spectra were obtained at The Ohio State University Campus Chemical Instrument Center (funded in part by National Science Foundation Grant 79-10019).

Registry No. I, 101032-01-3; I·C_6H_6, 101054-44-8; II, 101032-02-4; III, 101032-03-5; $(\mu$-H$)_2Os_3(CO)_{10}$, 41766-80-7; $[(\eta^5$-$C_5H_5)Mo(CO)_2]_2$, 56200-27-2.

Supplementary Material Available: Listing of anisotropic thermal parameters and structure factor amplitudes (73 pages). Ordering information is given on any masthead page.

(26) Churchill, M. R.; Hollander, F. J. *Inorg. Chem.* **1981**, *20*, 4124.

Communications

Trapping of a Reactive Tetraruthenium Imido Cluster with Diphenylacetylene

Margaret L. Blohm[1] and Wayne L. Gladfelter*[2]

Department of Chemistry, University of Minnesota Minneapolis, Minnesota 55455

Received December 10, 1985

Summary: Diphenylacetylene traps the intermediate imido cluster formed during the protonation of $[Ru_4N(CO)_{12}]^-$. Structural characterization of the new cluster $Ru_4(NH)(PhCCPh)(CO)_{11}$ revealed the first example of a tetrabridging imido ligand.

The reactivity of main-group atoms exposed along the edges or faces of metal clusters is receiving a great deal of attention. In particular it has been shown that the carbon atom in carbido clusters can be protonated,[3,4] alkylated,[5] and acylated[6] and also that CO can migrate from an adjacent metal onto the carbon to form a ketenylidene (CCO) ligand.[7] Fewer studies have reported chemistry of the nitrogen atom in nitrido clusters.[8] Recently, we reported spectroscopic evidence that the following protonation (eq 1) occurs via the intermediate imido cluster

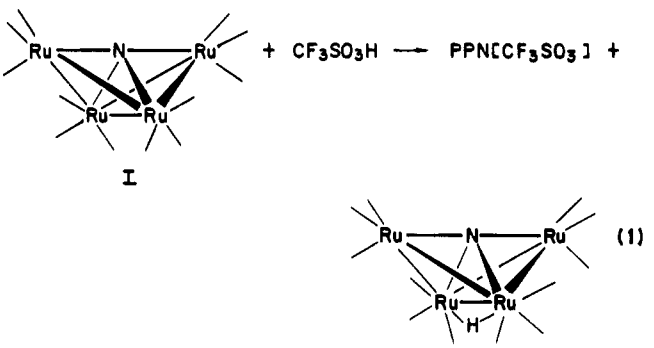

(1)

III.[9] Unfortunately, III could not be isolated as a crystalline solid. We have discovered, however, that diphenylacetylene is an effective reagent for trapping the spectroscopically observed intermediate in this protonation and that the product does indeed contain the first example of a stable μ_4–NH ligand.

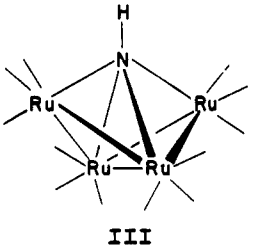

Addition of 1 equiv of CF_3SO_3H to a CH_2Cl_2 solution of $PPN[Ru_4N(CO)_{12}]$,[10] forms a bright purple solution. Immediate addition of excess diphenylacetylene (eq 2) to the purple intermediate results in the isolation of two

(1) NSF Predoctoral Fellow, 1982–1985.
(2) Alfred P. Sloan Fellow, 1983–1985.
(3) Tachikawa, M.; Muetterties, E. L. *J. Am. Chem. Soc.* **1979**, *101*, 7417.
(4) Hriljac, J. A.; Swepston, P. N.; Shriver, D. F. *Organometallics* **1985**, *4*, 158.
(5) Holt, E. M.; Whitmire, K. H.; Shriver, D. F. *J. Am. Chem. Soc.* **1982**, *104*, 5621.
(6) Davis, J. H.; Beno, M. A.; Williams, J. M.; Zimmie, J.; Tachikawa, M.; Muetterties, E. L. *Proc. Natl. Acad. Sci. U.S.A.* **1981**, *78*, 668.
(7) Kolis, J. W.; Holt, E. M.; Shriver, D. F. *J. Am. Chem. Soc.* **1983**, *105*, 7307.
(8) Gladfelter, W. L. *Adv. Organomet. Chem.* **1985**, *24*, 41.
(9) Blohm, M. L.; Fjare, D. E.; Gladfelter, W. L. *J. Am. Chem. Soc.*, in press.
(10) Blohm, M. L.; Gladfelter, W. L. *Organometallics* **1985**, *4*, 45.

0276-7333/86/2305-1049$01.50/0